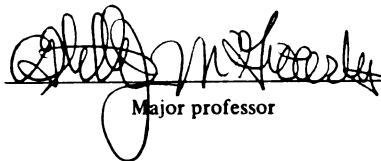This is to certify that the

thesis entitled

AN INVESTIGATION OF THE STRUCTURAL COMPONENTS
INVOLVED IN THE MECHANISM OF THE pH INDUCED SWITCH IN
THE CHANNEL SIZE OF OMPF PORIN FROM <u>E. COLI</u> K-12

presented by

John D. Roundtree

has been accepted towards fulfillment
of the requirements for

_____M.S._____degree in _Biochemistry_

<u>Major professor</u>

Date __8/24/98__

PLACE IN RETURN BOX to remove this checkout from your record.
TO AVOID FINES return on or before date due.
MAY BE RECALLED with earlier due date if requested.

DATE DUE	DATE DUE	DATE DUE

AN INVESTIGATION OF THE STRUCTURAL COMPONENTS INVOLVED IN THE MECHANISM OF THE pH INDUCED SWITCH IN THE CHANNEL SIZE OF OMPF PORIN FROM *E. COLI* K-12

By

John D. Roundtree

A THESIS

Submitted to
Michigan State University
In partial fulfillment of the requirements
for the degree of

MASTER OF SCIENCE

Department of Biochemistry

1998

ABSTRACT

AN INVESTIGATION OF THE STRUCTURAL COMPONENTS INVOLVED IN THE MECHANISM OF THE pH INDUCED SWITCH IN THE CHANNEL SIZE OF OMPF PORIN FROM *E. COLI* K-12

By

John D. Roundtree

It has been shown that the channel size of OmpF, a porin in the outer membrane of *Escherichia coli*, is dependent upon pH. The size of channels observed at acidic pH is approximately one half that observed at basic pH. Modification of OmpF with diethyl pyrocarbonate (DEPC) is known to lock the protein into the large channel configuration, regardless of pH. In this thesis, we show that Tyrosine 106 is the residue modified by DEPC. This is consistent with a conformational shift between two alternative structures for the protein. Using an artificial bilayer membrane assay (BLM), we analyzed the distribution of channel size at acidic and basic pH for several mutants of OmpF. A partial deletion of Loop 3 had a drastic effect on the size of the large channel, and only a slight effect on the small channel size. This shows that Loop 3 has a different role in defining the two channel sizes. Mutation of Tyrosine 106 to phenylalanine removed the DEPC sensitivity of OmpF, i.e. small channels were observed at acidic pH after the modification of the mutant OmpF with DEPC. Tyrosine 106 is located on Loop 3, providing additional evidence for involvement of Loop 3 in the conformational shift between the two channel sizes.

This is dedicated to my parents.

ACKNOWLEDGEMENTS

.

I would like to express my gratitude to the following people:

Dr. Estelle McGroarty for her patience and support.

Dr. Carrie Hiser for expertise, advice and friendship.

The members of my committee, Dr. John E. Wilson, Dr. Honggao Yan, and Dr. Leslie A. Kuhn for their help and interest.

TABLE OF CONTENTS

.

LIST OF TABLES

LIST OF FIGURES

LIST OF ABBREVIATIONS

BLM   Black lipid membrane or Bilayer lipid membrane

CHES   2-(N-cyclohexylamino) ethane sulfonic acid

Da   Daltons

DEPC   Diethyl pyrocarbonate

DNA   Deoxyribonucleic acid

EDTA   Ethylenediaminetetraacetate

FTIR   Fourier transformed infrared spectroscopy

kDa   Kilodaltons

LPS   Lipopolysaccharide

MDO   Membrane-derived oligosaccharide

Omp   Outer membrane protein

PAGE   Polyacrylamide gel electrophoresis

PEG   Polyethylene glycol

SDS   Sodium dodecyl sulfate

Tris   Tris (hydroxymethyl) aminomethane

VDAC   Voltage-dependent anion channel

INTRODUCTION

Literature Review

The cell envelope of Gram negative bacteria contains a double lipid bilayer system surrounding the cell, forming the interface between the cell and its environment [1]. The inner, or cytosolic membrane is a protein-rich phospholipid bilayer. It is the site for oxidative phosphorylation, the electron transport chain, active transport, and it is also critical for cell division [2]. The space between the inner membrane and the outer membrane is the periplasm. This space houses many nutrient scavenging proteins as well as a thin peptidoglycan layer [3-6].

The outer membrane is an asymmetric bilayer with lipopolysaccharide (LPS) comprising the outer leaflet [7-10]. The outer membrane functions as a protective barrier for the Gram-negative bacterium [11,12]. It is highly impermeable to hydrophobic compounds, although it allows for the passive diffusion of small, hydrophilic molecules [11,12]. The tight, quasi-crystalline packing array of the lipid and the consequent low fluidity of the LPS contribute to the outer membrane's low permeability [13-17].

LPS is comprised of three parts: the lipid A, the oligosaccharide core and the O-antigen [8]. Lipid A is a glucosamine disaccharide headgroup with typically, six fatty acyl chains in a combination of saturated and hydroxy fatty acids [8]. Attached to the lipid A is the oligosaccharide core. Studies of various mutant strains altered in the structure of the core have shown that extensive loss of the core sensitizes the bacteria to detergents and hydrophobic antibiotics [11,19,20]. The O-antigen is attached to the core, and extends into the medium. The O-antigen is comprised of up to 40 or more repeats of an oligosaccharide subunit [8]. The O-antigen is important for the bacterium to avoid

1

phagocytosis [18]. Strains which contain the O-antigen are referred to as smooth strains, and strains such as *Escherichia coli* K-12, which lack the O-antigen, are referred to as rough strains [8,11,12,18].

Very few types of protein are present in the outer membrane. Examples of minor protein components of the outer membrane include a number of proteases [21], a phospholipase [22], and several nutrient-specific transport proteins [11,23,24] of which there are only a few hundred copies of each per cell [11,21-24]. Murein lipoprotein is the most abundant protein in the outer membrane at 7×10^5 copies per cell [11]. Lipoprotein anchors the outer membrane to the peptidoglycan layer by covalently linking the inner lipids to the peptidoglycan [25]. OmpA is another prominent protein component of the outer membrane, with 10^5 copies per cell [26]. Studies of mutant strains lacking OmpA have shown that the loss of this protein results in spheroid shaped cells instead of the wild type rod shape, as well as in a less stable outer membrane [11]. OmpA has been attributed with a channel-forming capacity [27], although the channel of OmpA has a much slower rate of diffusion than the other major class of outer membrane proteins, the porins [28]. The porins are the main channel-forming proteins responsible for the passive transport of molecules across the outer membrane and afford the structure its permeability to small (<600 Da), hydrophilic molecules [29-32]. Porins have been shown to be critical for the passage of nutrients across the outer membrane [33].

Typical enteric bacteria have several porins that are differentially expressed based upon environmental factors [11,34-38]. The four porins of *E. coli* are OmpC, OmpF, PhoE and LamB or maltoporin [39,40]. OmpC, OmpF and PhoE are general diffusion porins with slight ion selectivities [41], and the three share 60% sequence identity [42].

2

OmpC and OmpF exhibit slight cation selectivity [11,41], while PhoE is slightly anion selective [11, 41]. LamB can function as a general diffusion channel, but specifically facilitates the uptake of maltose and maltodextrans [11,43], whose presence is required for the induced expression of the LamB protein [44,45]. OmpC and OmpF are synthesized in very high amounts but are differentially expressed depending on temperature, osmolarity and pH [11,35,46]. At basic pH [46], low osmolarity and low temperatures (30°C), OmpF is preferentially expressed [11,35] and at acidic pH [46], high osmolarity and high temperatures (37°C), OmpC is produced in high amounts [11,35]. PhoE is expressed under conditions of phosphate starvation [11,47], although it does not show preference for passage of phosphate over other anions [48]. There are a total of 10^5 porin molecules per cell [49]. Regardless of environmental conditions, the outer membrane's total content of porin remains essentially constant [39,50,51].

The crystal structures of OmpF from *E. coli* [52] and the major porin of *Rhodobacter capsulata* [53-55] have been defined and are very similar in geometry, although the two share no sequence homology [56]. These two structures have been used to define the classical porin structure [57-59], although the porin class extends to more than just Gram-negative bacteria, since similar proteins are found in some organelles such as mitochondria [60] and chloroplasts [61]. There are examples of monomeric porin-like proteins such as OmpA [27] and the major porin of *Pseudomonas aeruginosa* [62], but the protein is generally arranged in trimers with each of the three peptides forming its own independent transmembrane, water-filled channel [52-55]. The basic architecture of each monomer is a sixteen stranded amphipathic β-barrel (Figures 1 and 2), with the internal face of the barrel being hydrophilic and the external face being

hydrophobic. There are two belts of aromatic side chains facing the exterior of the protein, one near the periplasmic end of the barrel and one near the extracellular face [52-55,63]. These rings are thought to be important for the stabilization of the protein-protein interactions within the trimer as well as the orientation of the trimer with respect to the bilayer [63]. The turns, which connect the strands on the periplasmic face of the protein, are only one or two residues in length. In contrast, the loops on the extracellular face of the protein are quite long. One loop (Loop 3) folds down into the channel along one wall and contributes to the constriction zone of the channel, or the so-called 'eyelet region' which is close to the midpoint of the bilayer [52-55]. The constriction zone of the channel is located at about the midpoint of the channel, parallel with the plane of the bilayer [52-55]. In the crystal structure of OmpF, the opening of the eyelet is roughly oval with dimensions of 7x11 Å [52]. The eyelet (Figure 2, A and B) is composed of positively and negatively charged groups which are arranged in an asymmetric geometry, with the positive side being comprised of three tightly stacked arginines (R42, R82, R132), in an arrangement which maximizes their π bonding interactions [52, 64]. Several other arginines and lysines are located near the region but are not directly in the eyelet [52, 64]. Several negatively charged acidic amino acids extend from Loop 3 opposite the channel from the arginine cluster (Figure 2C) [52]. Several tyrosines (e.g., Y40, Y106, and Y310) are also part of the constriction zone, with their hydroxyl groups contributing to the polar characteristics of the eyelet [52].

It is presumed that the exclusion limit of the pore is related to the structure of the eyelet region, which forms the narrowest passage of the channel [57]. Selection for growth on carbon sources larger than the exclusion limit of wild type porin resulted in

Figure 1. The ribbon representation for a monomer of OmpF shows the basic architecture for the porins of Gram-negative bacteria [52]. The arrows (1-16) indicate the β-strands which form the walls of the barrel structure. The short turns (T1-T8) are located on the periplasmic face of the protein. The long loops (L1-L8) form the extracellular face of the channel, with the exception of Loop 3 (L3). Loop 3 folds into the channel and contributes to the constriction zone of the pore.
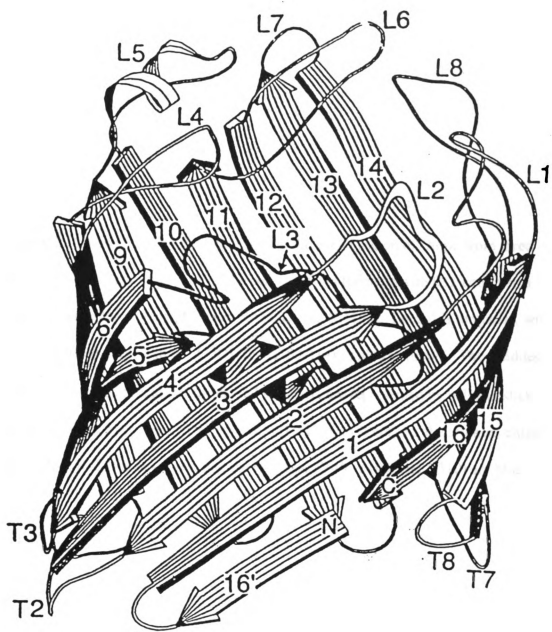
Figure 1

Figure 2. Cutaway ribbon diagrams present the eyelet region of OmpF from three

different viewpoints: from outside the cell (A), from the periplasm (B), and from a

position inside the channel, between R42 and R82 (C) [52]. Loop 3 is turquoise, with the

portion deleted in the OmpF of OC1508 (Δ109-114) shaded in purple. The residues that

comprise the eyelet region of the crystal structure, are represented by ball and stick

models without hydrogens. The aspartates (D113, D117) are red, the arginine cluster

(R42, R82, R132) is in yellow, and the tyrosines (Y40, Y106, and Y310) are blue.

A

B

C

Figure 2

8
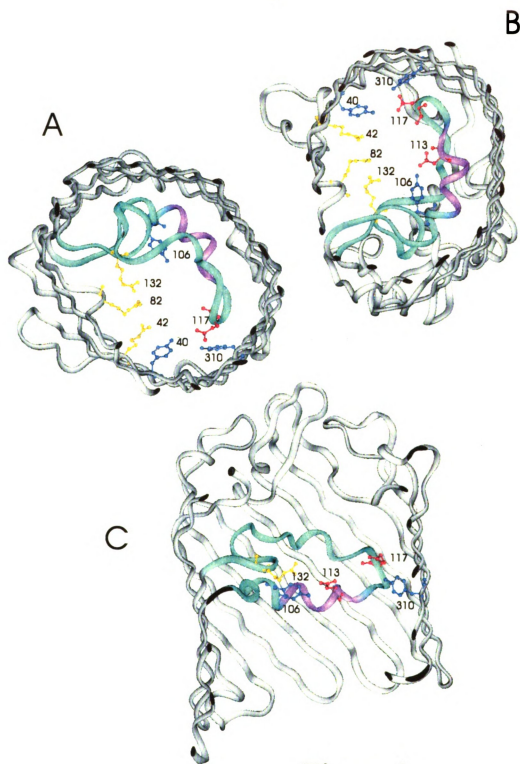
point and deletion mutants in the constriction zones of OmpF and OmpC [65-68]. The point mutants which were generated, were charge to neutral mutations. The deletion mutants were in Loop 3, and resulted in the removal of one or more charged groups in the eyelet, along with some of the bulk which constricted the channel. These mutants not only allowed for the passage of larger molecules in multi-lamellar liposome swelling assays, they also resulted in increased sensitivity of the cell to detergents and some anitbiotics [65-68].

A black lipid membrane (BLM) apparatus can be used to investigate the functionality of channel forming proteins *in vitro* using an artificial bilayer with a fixed transmembrane potential [69-71]. The typical BLM is comprised of two chambers which are filled with a buffered salt solution, and the only connection between the two chambers is through a small hole on which the bilayer is formed. This assay system measures channel openings or insertions as increases in the electrical conductance across the bilayer. The increase in conductance observed for the insertion of a porin into the bilayer is proportional to the cross-sectional area of the channel [69-71], because the ion flow through the channel resembles the flow of ions in free solution [71-73]. BLM data can be used to compare the channel sizes in a relative manner, but do not allow for accurate calculation of the actual diameter of the channel [74].

BLM studies of the OmpF mutants discussed above have shown that the residues R42, R82, R132, D113 and a portion of Loop 3 (109-114), which comprise the constriction zone of the channel, are involved in the ion selectivity displayed by different porins [75]. The OmpF porin mutants in which a negative charge is replaced with a neutral amino acid in the eyelet region have been reported to have decreased cation

selectivity, while charge to neutral mutations in the arginine cluster (R42, R82, R132) increase the cation selectivity [75]. In a colicin-resistant mutant of OmpF, the substitution of a negatively charged group for a neutral amino acid (G119D) on Loop 3 gives the channel a higher cation selectivity, although the additional bulk appears to reduce the overall size of the pore [76]. The role of the constriction zone in channel specificity is thought to be broader than just ion selectivity. The residues comprising the eyelet region of LamB form the binding site for maltodextran [77]; so, in general, it may be that channel specificities are determined at the constriction zone [57].

It has been shown that the open state of porins is voltage dependent [69, 78-81], with the channels gating shut at high voltages. The porins of Gram-negative bacteria reportedly gate closed at potentials greater than 100-150 mV [69, 78-81]. The mechanism for gating has not been determined, but has been proposed to include either the protonation of a particular residue restricting the flow of ions or the closure of a protein lid [57, 63]. The threshold for voltage gating is much higher than the expected Donnan potential (30 mV) [82], raising doubts about the physiological relevance of voltage gating [83]. It has been argued by Lakey and colleagues, however, that in dilute solutions the local Donnan potential between the extracellular solution and the periplasmic space could reach as high as 130 mV [84]. Components of the periplasm and the outer membrane, such as membrane-derived oligosaccharides (MDO) [85], and polycations [86], have been shown to lower the threshold of voltage gating *in vitro*, suggesting that the cell may be able to regulate the voltage gating activity of its porin [85,86].

The gating of OmpF and OmpC has been shown to be sensitive to pH with a titration point at about neutral pH [75,80]. At acidic pH, the channel reportedly gates closed much more readily than at basic pH [75, 80]. The charge to neutral mutants in the eyelet region of OmpF as well as the short Loop 3 deletion mutant of OmpF (Δ109-114), which affect ion selectivity, also are reported to remove the pH sensitivity of the gate [75]. Point mutations in the arginine cluster result in channels that have lower voltage thresholds for gating [75]. The mutant D113G is reported to have a modest increase in its voltage threshold for gating [75]. The colicin-resistant mutant, G119D, which has a neutral to negative mutation in the eyelet, has been shown to have an increased voltage threshold for gating by almost twofold [76].

The channel size of porin also has been reported to have a pH dependency [87]. Porins OmpF, OmpC and PhoE have been shown to have two substates of the open state, the stability of which are dependent upon the pH of the bathing solution. At basic pH the channels have a size corresponding to the literature values, as determined by both BLM and liposome swelling assays. At acidic pH, the channels are roughly one half the size of the large channels observed at basic pH. The presence of two distinct, pH-dependent channel sizes is observed in both BLM and liposome swelling assays. The size switch was shown to occur over a very narrow range, close to neutral pH. OmpF titrates with a midpoint at 7.5, and OmpC titrates at pH 6.5 (Figure 3) [87].

The lone conserved histidine amongst the three porins was investigated as a potential structural component of the pH sensor since its R group titrates in the neutral range. The investigators proposed a model utilizing the histidine as the pH sensor for the

11

Figure 3. The titration curves for the large channel size for OmpC (A) and OmpF (B),

show that the switch in channel size occurs at neutral pH for each of them [87]. At basic

pH mostly large channels are observed. At acidic pH's, small channels are observed,

indicated by the decreased amount of large channel in the two titration curves.
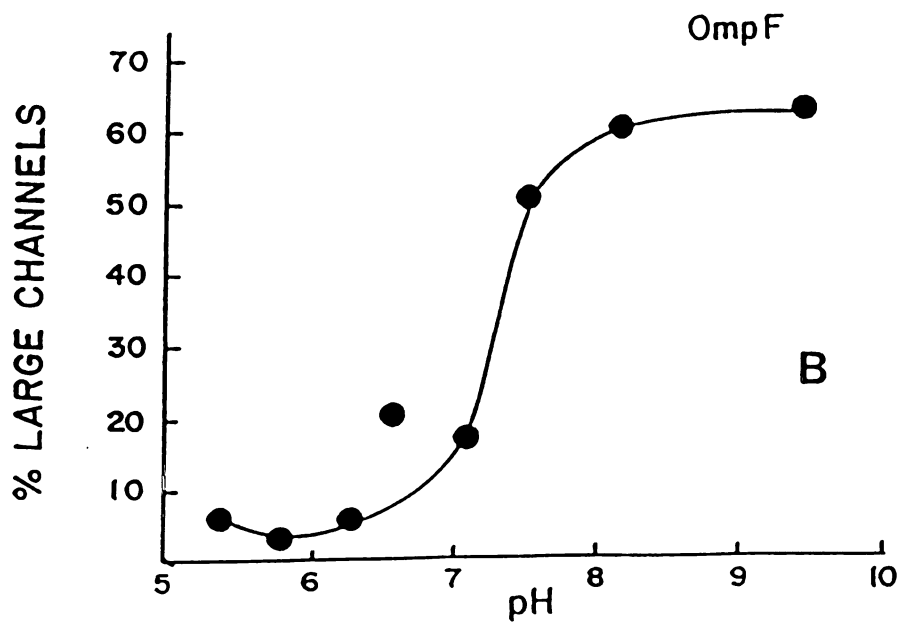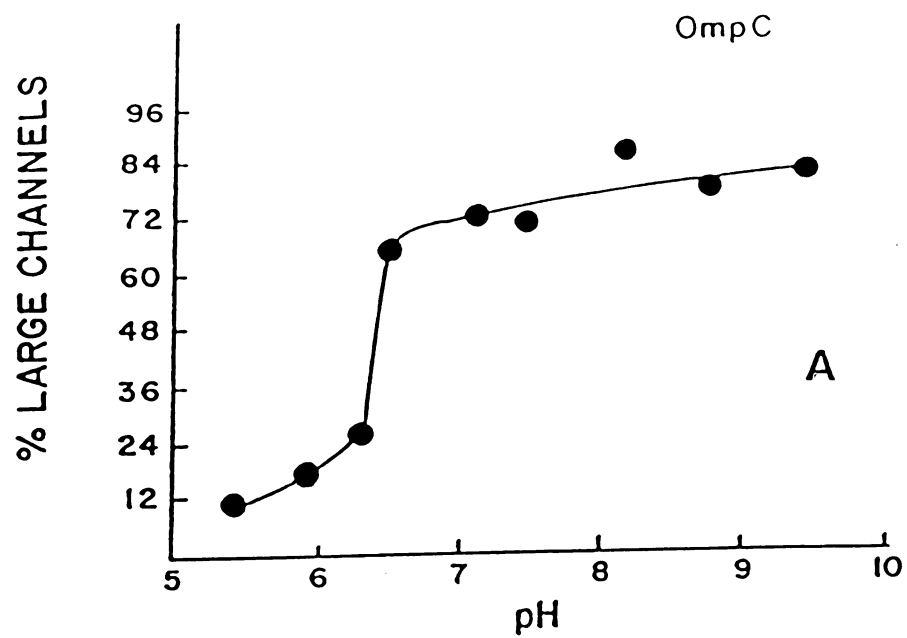
Figure 3

Figure 4. The probability distribution histograms of the size parameter, λ/σ, for unmodified OmpF at acidic (A) and basic (B) pH, and DEPC-modified OmpF at acidic (C) and basic pH (D) show that modification with DEPC removes the presence of small channel at acidic pH [88]. Reversal of the modification with hydroxylamine restores the presence of small channels at low pH (E). P is the percentage of the total observed channels of a certain size. The size parameter, λ/σ, has units of Å.
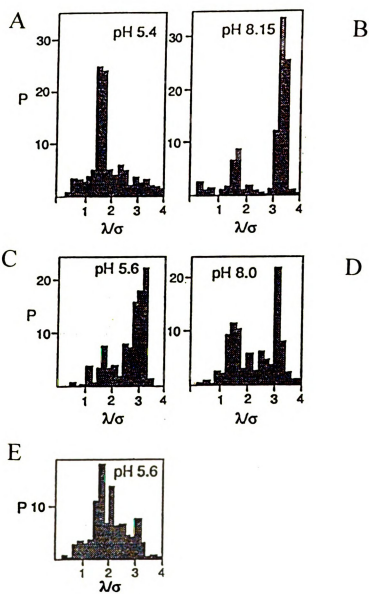
Figure 4

channel size switch [88]. According to this model, the side chain would be neutral at basic pH and the large channel size would be favored because the large channel conformation of the protein would be stabilized. At acidic pH, the histidine would be positively charged which would induce a conformational shift to form a small channel, most likely stabilized through favorable electrostatic interactions between the positively charged histidine and a negatively charged residue(s). To test this model, the investigators used diethyl pyrocarbonate (DEPC) to chemically modify the histidine residue. The carbethoxylated side chain would be neutral at both basic and acidic pH's, removing the titratable character of the histidine. DEPC was chosen as a reactant because it shows much higher specificity for histidine than for other side chains [88,89]. If the modification can be reversed with the addition of hydroxylamine, then the modified residue was most likely a histidine, with a slight possibility that it could be a tyrosine [89]. The modification of porin with DEPC resulted in the presence of large channels at acidic pH (Figure 4C) [88]. Hydroxylamine was used to reverse the modification of the carbethoxylated protein and the effect of DEPC modification was reversed, i.e. small channels were observed at acidic pH again (Figure 4D) [88]. This result fits the prescribed model for the histidine as the pH sensor, because the carbethoxylated side chain is neutral and the observed channels are large, independent of the pH. The modification essentially locked the protein into the large channel conformation. However, in the crystal structure of OmpF, the histidine is located outside the channel in the belt of aromatic residues surrounding the extracellular face of the protein at the subunit/lipid interface [52]. This location of the histidine coupled with the DEPC's

16

capacity to cross-react with tyrosine residues, has called into question the role of the histidine as the pH sensor for the switch in channel size [64,89,90].

Another chemical modification experiment supports a model for a pH dependent conformational shift in the structure of porin. Differential modification of lysines in OmpF over a large span of pH's revealed altered accessibility to several residues in the channel at various pH's. The investigators suggested that pH dependent structural rearrangements of the protein were responsible for the variable accessibilities of the lysine residues to modification [91].

Other than the two chemical modification experiments, there has been very little insight into the structural differences between the multiple conformations of porin. Fourier transformed infrared spectroscopy (FTIR) was used to analyze the secondary structure of OmpC and OmpF at both acidic and basic conditions [88]. No change in the secondary structure of the protein was detected over the range of pH in which the switch between the two proposed channel conformations occurs [88].

Research Project Goals

The mechanisms controlling the voltage gating activity of porin and its pH dependency have been attributed to several residues in the eyelet region of the channel. However, the pH-dependent channel size switch of the porins of *E. coli* has not been examined extensively to identify the structural component(s) of the protein which are involved in this proposed conformational shift. The objective of this thesis is to define the amino acid that is the site for carboxyethylation by DEPC, and examine that residue's role in a proposed mechanism for the pH-induced switching between the substates of the open channel.

MATERIALS AND METHODS

Materials

The *E. coli* K-12 strains, OC904, IB914, and OC1555, were provided by Spencer Benson [68,95]. The wild type OmpF gene was cloned from the *E. coli* K-12 strain PLB3261 and was also provided by Spencer Benson [68]. Molecular procedures were carried out with the Mutagene Phagemid *In Vitro* Mutagenesis kit (Bio-Rad). The porinless *E. coli* strain, UH302 used in the expression system for wild type and mutant OmpF porin in this study, was provided by Ulf Henning [92]. Diphantonoyl phosphatidylcholine used in the BLM studies was purchased from Avanti Polar Lipids. Diethyl pyrocarbonate was obtained from Sigma. Molecular weight markers were purchased from Sigma. Oligonucleotide primers were synthesized by the Macromolecular Structure Facility at Michigan State University. DNA sequencing was performed by the MSU DNA Sequencing Facility at Michigan State University.

Expression of Wild Type OmpF in UH302 and Site-Directed Mutagenesis

The molecular procedures were performed almost entirely by Dr. Carrie Hiser [93,94]. The wild type OmpF gene was PCR-amplified directly from a crude extract of chromosomal DNA from PLB3261 and cloned into pUC119. Site-directed mutagenesis was performed as described in the Mutagene Phagemid *In Vitro* Mutagenesis Kit. The expression vector was a modified version of the pTrc99A plasmid (Pharmacia), which had been altered to remove a ribosome binding site and alternative start codon upstream from the site of insertion for the OmpF gene. The transformation of UH302 cells with the OmpF containing pTrc99A plasmid required that the ligation mix in the final step of the mutagenesis protocol not include polyethylene glycol (PEG) or that the plasmid first

be transformed into XL1-Blue cells (Stratagene), before isolating the plasmid to transform UH302 cells [92]. Oligonucleotide primers obtained from the Macromolecular Structure Facility for the generation of H21A and Y106F were (5' to 3'): for H21A, CTGTTGGGCTAGCTTATTTTTCC, and for Y106F, GTGTGGTTTTTGATGCCCTAGGTTACACC.

Cell Growth

OmpF wild type porin was isolated from *E. coli* strain PLB 3261, which lacks LamB and OmpC, and also from WT/pAtrc/UH302. The *E. coli* UH302 strain lacks all porins and was used to express wild type as well as mutant porins [93,94]. The UH302 derived strains and those strains provided by Spencer Benson were grown in 1% tryptone, 0.5% yeast extract. Cells were grown at 30°C and were harvested after overnight growth. All strains used in this study are listed in Table I.

Table I. *E. coli* Strains used in this Study.

Strain	Porin Mutant	Reference
OC904	D113G	95
IB914	R132L	95
OC1555	Δ114-129	68
WT/pAtrc/UH302	Wild Type	93
H21A/pAtrc/UH302	H21A	93
Y106F/pAtrc/UH302	Y106F	94
PLB3261	Wild Type	68
UH302	Porinless Strain	92

Porin Isolation

Porins were isolated according to the method of Lakey, et al. [84,87] with some modification. A French press was used to break the cells, which were then treated with RNase and DNase. After the membranes were pelleted at 100,000g, the inner membrane was dissolved with 2% sodium dodecyl sulfate (SDS), 10 mM Tris, pH 7.5. Following centrifugation, the pellet contained the outer membrane and peptidoglycan layer with the bound outer membrane proteins, which include porin. The porin was solubilized with 0.5 M NaCl in the presence of 0.7 M mercaptoethanol and 5 mM ethylenediamino-tetraacetic acid (EDTA) in 2% SDS, 10 mM Tris, pH 7.5. The solubilized porin was dialyzed against 10 mM sodium bicarbonate, pH 8.0, and precipitated with 90% acetone at 4°C [84,87]. Homogeneity of the porin was assessed by SDS-PAGE (sodium dodecyl sulfate-polyacrylamide gel electrophoresis) using the method of Laemmli [96]. The final preparation of porin was suspended in 1%SDS, 10 mM Tris, pH 6.8 and 0.02% sodium azide [84,87].

Gel Electrophoresis

The purity of the porin samples was analyzed by SDS-PAGE. Samples were run in a minigel apparatus using a separating gel of 12% polyacrylamide and a stacking gel of 5% polyacrylamide. The minigels were run at 10 mA and then 20 mA as the sample began to enter the separating gel. The gels were stained with Coomassie brilliant blue to detect the protein bands. A sample was considered pure if the non-porin bands were estimated to be less than 5% of the total protein on the gel. Those samples that had

significant protein contamination, were further purified on a Sephadex G-200 column [87].

Temperature Stability Assessment

The overall stability of wild type and mutant OmpF isolates was assessed by the presence of the unfolded monomer of OmpF in the sample after a heating step. In this experiment, 100 μl samples of wild type and mutant OmpF porin were mixed at 0.25 mg/ml with a 1:1 dilution with the sample buffer. The samples were then heated in a water bath for one minute at a prescribed temperature, after which they were transferred directly to a room temperature water bath to cool. Then the samples were loaded onto a SDS-PAGE unit similar to the one used for assessing sample purity. Electrophoresis was performed on a larger gel system with a constant voltage of 15 mA until the samples were entering the running gel, at which point the voltage was increased to 30 mA. Coomassie blue was used to stain the protein bands [97,98].

Bilayer Membrane Assay (BLM)

Porin channel size was measured by analysis of electrical conductance across a bilayer lipid membrane under various conditions. The membrane was formed with a solution of 1% diphytanoyl phosphatidylcholine in n-decane. A small volume of porin was added to each side of the salt solution bathing the membrane. This bathing solution contained 0.5 M NaCl in 1 mM of the appropriate buffer (CHES was used for pH 8-8.5, and succinate for pH 5.4-7.0). Silver-silver chloride electrodes were placed on either side of the membrane and normally a constant voltage of 50 mV was applied using a 1.5 V battery, although other voltages were examined. Changes in current were amplified using a Keithley Model 614 electrometer and recorded [87,88]. The changes in current were

reported as the size parameter, λ/σ, which is proportional to the cross-sectional area of the pore [71-73]. A statistically significant number of channels (>200) were analyzed for each experimental condition.

Modification of Porin with DEPC

Carbethoxylation of isolated OmpF with DEPC was performed in 20 mM phosphate buffer, 0.5% SDS, pH 7.5, according to the method of Bindslev and Wright with some modification [88,95]. A DEPC stock solution was prepared immediately prior to use by diluting an aqueous solution of DEPC with equal volumes of anhydrous ethanol and determining the actual DEPC concentration by quantitative dilution of a small aliquot (1-5μl) into 3 ml of 10 mM imidazole, pH 7.5. The absorbance at 230 nm of this solution, was converted to DEPC concentration using an extinction coefficient of 3000 cm^{-1}M^{-1}. A 1 ml aliquot of a 0.5-2.0 mg/ml solution of porin was modified by the addition of 1-2 μl of DEPC stock solution at a ratio of 18.5-80 mol of DEPC/ mol of porin [88].

RESULTS

Isolation of Porin and Purity Determination of Isolate

Wild type OmpF porin was isolated from both PLB 3261 and WT/pAtrc/UH302. The mutant porins of OmpF, H21A and Y106F, were isolated from H21A/pAtrc/UH302 and Y106F/pAtrc/UH302, respectively. The D113G, R132L, and Δ114-129 mutant porins were isolated from strains OC904, IB914, and OC1555, respectively. The purity of the isolated porin was assessed from Coomassie blue staining of gels from SDS-PAGE (data not shown.)

Temperature Stability of Isolated Porin

The folded trimer is much larger than the 37 kDa monomer of OmpF and does not migrate as far on the gel as the monomer. The multiple banding pattern observed for the folded trimer of some of the samples reflects variable amounts of bound LPS [97,98]. Porin which is LPS-enriched is more stable to higher temperatures than its LPS-depleted counterpart [97,98]. The samples of wild type, H21A, Y106F, and R132L OmpF porins show the multiple banding patterns indicative of LPS-enriched porin (Figure 5). The OC1555 and D113G porin isolates do not have this banding pattern, indicating that they have been stripped of most of the bound LPS (Figure 5).

Under the given conditions, wild type OmpF porin denatured at approximately 70-75°C. The R132L point mutation did not decrease the temperature stability of the protein, however the other mutations investigated in this study resulted in proteins that unfolded at lower temperatures relative to wild type. The temperature stabilities of the porin isolates are listed in Table II.

Figure 5. A 12% acrylamide SDS gel depicting the thermal stability of wild type OmpF

and the OmpF mutants used in this study. Each porin was heated for one minute at each

temperature and then cooled to room temperature before loading onto the gel. Seven

temperatures were used for each porin isolate. Lanes labeled (a) were treated at 50 °C;

(b), 55 °C; (c), 60 °C; (d), 65 °C; (e), 70 °C; (f), 75 °C; (g), 100 °C. Lane (x) contains the

molecular weight markers. The multiple banding pattern of the folded trimer, as seen in

lane (a) of wild type, is due to the variable amounts of LPS bound to the porin. The heat

denatured protein runs as a monomer, as seen in lane (g) for each porin.
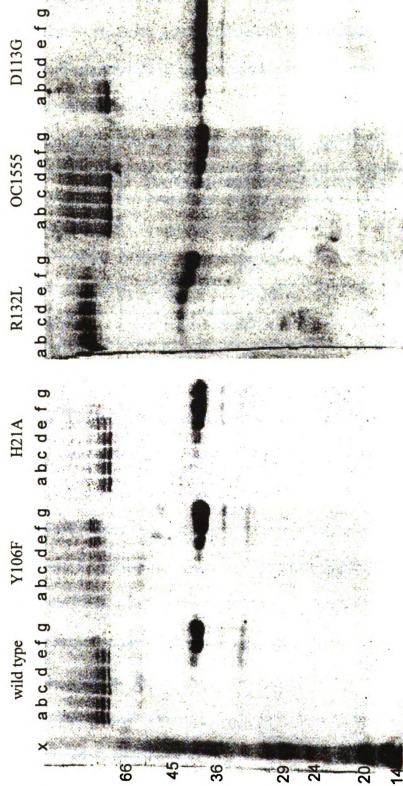
Figure 5

The interpretation of the temperature stability of OC1555 and D113G is complicated because these two samples were LPS-depleted, while the wild type OmpF control was LPS-enriched. However, a valid comparison between the two mutants can be made, showing that LPS-depleted D113G OmpF unfolds at a temperature approximately 10°C less than the OmpF porin of OC1555.

Table II. Temperature Stability for Wild Type and Mutant OmpF Porin.

Mutation	Maximum Temperature Stability (°C)
Wild Type	70-75
Y106F	65-70
H21A	65-70
R132L	70-75
OC1555 (Δ114-129)	65
D113G	55

The Effects of pH on the Channel Size Distribution for Several Porin Mutants

It has been previously documented that the channel size of the *E. coli* porins OmpF, OmpC and PhoE, is dependent upon pH [87]. At constant voltage, the stepwise increases in conductance (Figure 6) reflects the size of the channel as porin inserts into the membrane, allowing for the increase in ion flow across the membrane. The size of a channel observed in the BLM assay is reported as the size parameter, λ/σ, where λ is the incremental increase in conductance of each channel opening event and σ is the specific conductance of the salt solution. This size parameter has units of $\overset{\circ}{A}$, and is proportional to the size of the channel, although it is not an accurate measure for the absolute size of the channel [12,74]. BLM measurements are used for comparisons in a qualitative sense [74,87]. From my data, the calculated λ/σ for the most observed channel size for wild

Figure 6. The stepwise increases in current across a membrane comprised of 1%

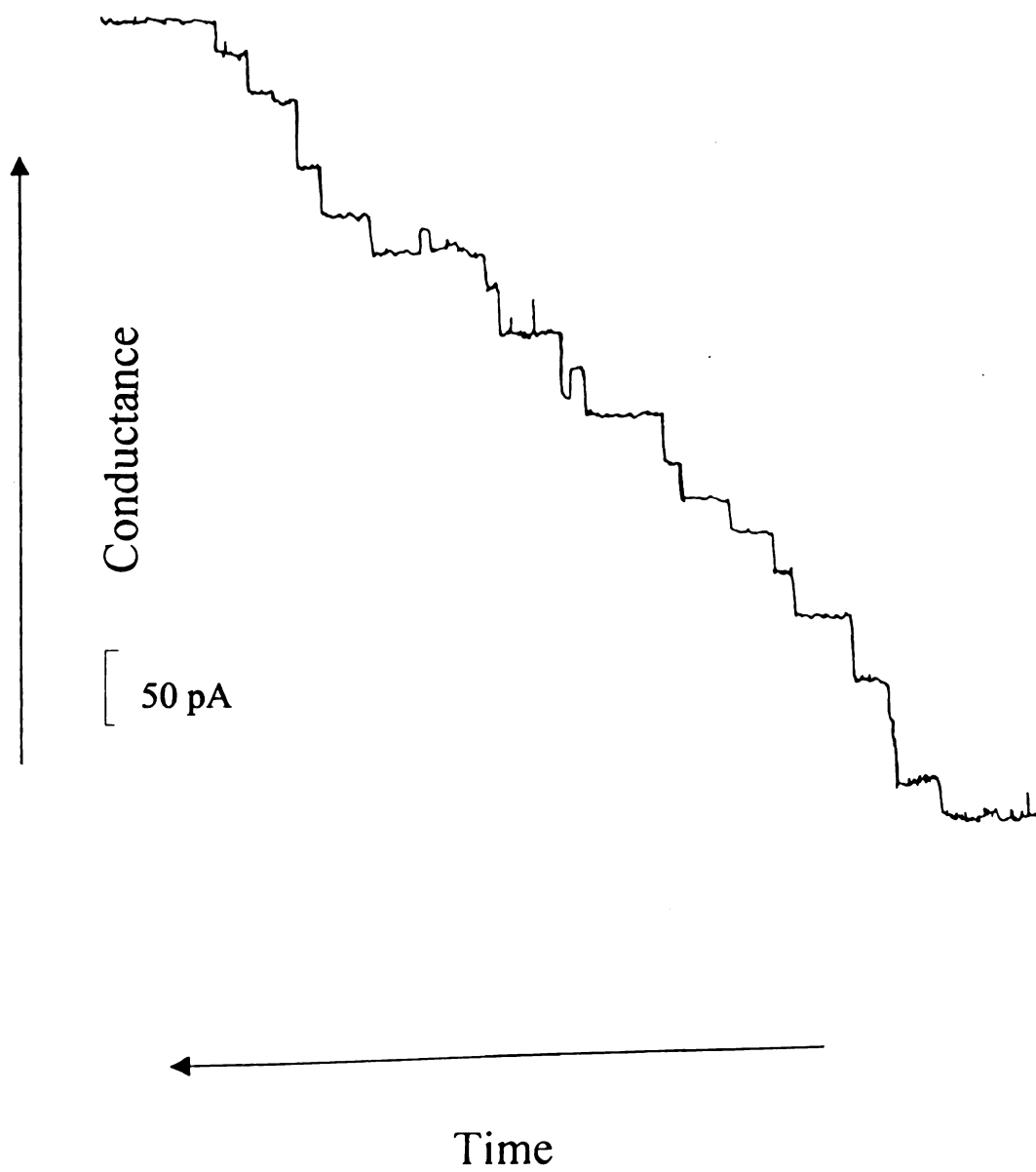diphantonoylphosphatidylcholine correlate to the insertion of channels into the bilayer.

Figure 6

type OmpF at pH 8.5 is 2.9-3.3 Å, while the calculated λ/σ for wild type OmpF at pH 5.4

is 1.5-1.7 Å, taken from the histograms in Figure 7. This is consistent with the previous

finding that the small channel of OmpF normally has a λ/σ calculated to be 1.5-1.7 Å and

a large channel of 3.1-3.7 Å [87,88].

Table III. Observed λ/σ for Mutant Porins at Acidic and Basic pH.

Mutant	λ/σ, acidic pH[a] (Å)	λ/σ, basic pH[b] (Å)
Wild Type	1.5-1.7	2.9-3.3
H21A	1.7	3.1
Y106F	1.7	1.5-1.7, 2.9-3.3
R132L	1.5-1.7	2.9-3.1
D113G	Not done	2.9-3.1
OC1555 (Δ114-129)	1.3-1.5	1.9-2.1

[a]Acidic pH range was normally adjusted to pH 5.4-7.0.

[b]Basic pH range was normally adjusted to 8.0-8.5.

To further test the model for the histidine as the pH sensor for the size switch, the

OmpF mutant H21A was generated [93]. In my experiments, the BLM data for H21A

(Figure 7, C and D) shows a channel size distribution similar to wild type OmpF, with a

predominant small channel size, λ/σ of 1.7 Å at low pH and a predominant large channel

size, λ/σ of 3.1 Å at basic pH. This result is not consistent with a model requiring a

positively charged histidine 21 in order to form small channel and suggests that the

histidine is not the pH sensor for the size switch. In addition, I repeated the DEPC

modification experiments using the OmpF mutant H21A. The histogram of the data

(Figure 9B) shows that large channels are predominantly observed at acidic pH. This

indicates that the DEPC effect upon channel size is independent of the histidine residue.

Figure 7. The probability distribution histograms of channel size for wild type OmpF (Panels A and B) and the point mutants, H21A (Panels C and D) and Y106F (Panels E and F), at acidic and basic pH as measured in an artificial bilayer membrane assay (BLM). Only opening events were used to calculate the percentage of channels observed at a certain size range. Electrical conductance across the bilayer was measured while the potential across the membrane was held constant. The porins were added on each side of the membrane, into the bathing solution of 0.5 M NaCl buffered with 1 mM of the appropriate buffer (CHES for pH 8.0, and succinate for pH 5.4). λ is the incremental increase in conductance observed for each channel insertion, and σ is the specific conductance of the bathing solution. The size parameter has units of Å, and is proportional to the narrowest point of the channel.
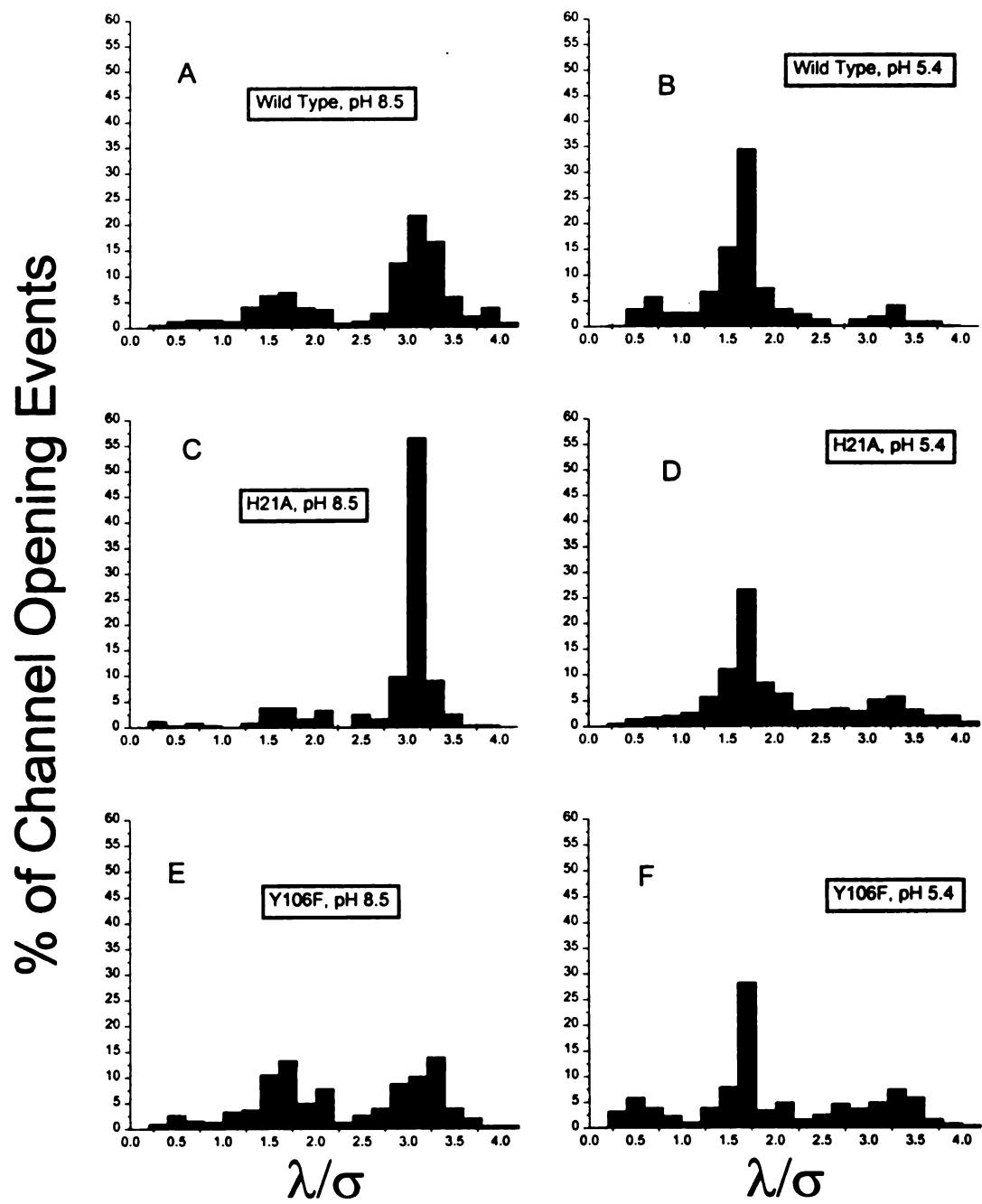
Figure 7

Figure 8. Probability distribution histograms of channel size for three OmpF mutants; D113G (Panel A), R132L (Panels B and C)and the partial Loop 3 deletion OmpF mutant, OC1555 (Δ114-129) (Panels D and E). The experiment was carried out as described in Figure 1.
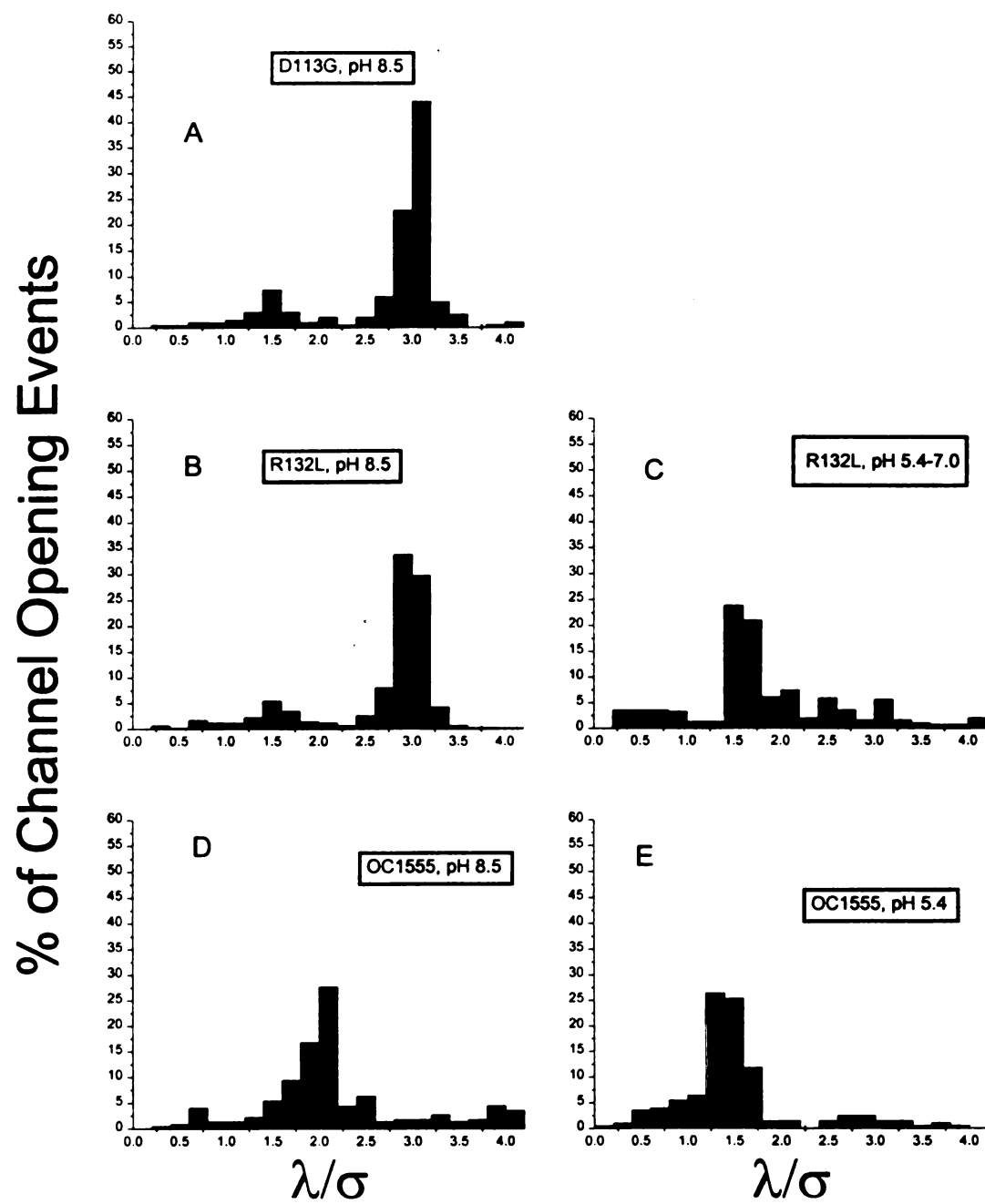
Figure 8

Figure 9. Probability distribution histograms of the channel size for DEPC-modified

wild type OmpF (Panel A) [88], DEPC-modified H21A (Panel B), and DEPC-modified

Y106F (Panel C) at pH 5.4 as measured in the BLM. This experiment was conducted in

the same manner as described in Figure 1, except for the use of DEPC modified porin

which was measured at only acidic pH.

Figure 9

Given that hydroxylamine can restore wild type behavior to the modified wild type OmpF [88] and that the only histidine in the protein is not required for the modification to lock the protein into large channel conformation, a tyrosine is the most likely candidate for the DEPC modification [89]. Mutations that allow for the passage of large maltodextrans, were all localized to the residues wh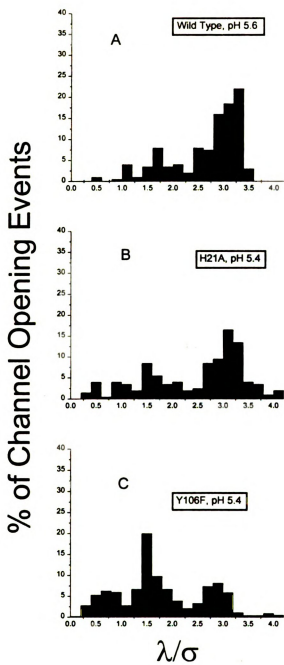ich contribute to the eyelet region of the channel [52, 65-68,100]. These mutant porins also have altered ion selectivity and voltage gating properties [75]. These findings point to the eyelet region of the protein as the most likely site for altering channel size. Tyrosines are not typically reactive with DEPC [89], so the tyrosine involved in the modification reaction would most likely be involved in an interaction that increased the nucleophilic character of the hydroxyl group. Y106 is located on the α-helical portion of Loop 3, with its side chain extending into the channel, contributing to the eyelet region of the channel, as shown in Figure 2. In the crystal structure, the hydroxyl of Y106 and the side chain of D113 are oriented with a distance, and bond angles that favor a hydrogen bond between the two [52]. Such an interaction would increase the nucleophilicity of the hydroxyl group. The OmpF mutant Y106F was generated [94] because it is a conservative mutation that only removes the hydroxyl from the phenyl ring.

The channel size for the Y106F mutant porin was assessed at acidic and basic pH's using the BLM. My experiments show that the size of the channels for the Y106F porin at acidic pH is similar to the channel size of wild type OmpF under the same conditions, with the predominant observed channel size being λ/σ of 1.7 Å (Figure 7F). The channel distribution of Y106F at basic pH (Figure 7E) does not have a distinct single channel size. This disruption of the channel size at basic pH is not due to the loss of the

Y106-D113 hydrogen bond, because the mutant D113G has a prominent large channel size (λ/σ) of 3.1 Å at basic pH (Figure 8A).

The channel size distribution in the histogram of DEPC-modified Y106F at low pH (Figure 9C) is similar to that of unmodified Y106F at low pH. The most observed channel size (λ/σ) for the DEPC-modified Y106F is 1.5 Å. The porin from the Y106F mutant is still capable of forming small channels even after reaction with DEPC, suggesting that Y106 is required for the DEPC modification to lock the channel into the large channel conformation.

Y106 is located on Loop 3. The DEPC experiments suggest that Y106 plays a role in the channel size switch, which indicates that Loop 3 might be involved in the formation of small channel. OC1555 (Δ114-129) is an OmpF deletion mutant, which has a large portion of Loop 3 removed [68]. In my BLM experiments, the observed channel size distributions of OC1555 (Figure 8, B and C) differ from wild type OmpF. At acidic pH, the predominant channel size (λ/σ) observed for OC1555 OmpF is 1.3-1.5 Å. This is only slightly smaller than the small channel size of wild type OmpF, at (λ/σ) 1.7 Å. The predominant channel size observed at basic pH for OC1555 is (λ/σ) 1.9–2.1 Å, which is two-thirds the size of the channels observed for wild type OmpF at basic pH. According to this data, a large deletion of Loop 3 has resulted in smaller channel size (λ/σ), as observed in BLM assays. However, this mutation allows for growth on maltodextrans larger than the exclusion limit for wild type OmpF [68], implying a larger channel, in contradiction with the BLM data. This contradiction between BLM and *in vivo* studies has been observed for other OmpF mutants as well [75]. The smaller channel size

observed in the BLM has been proposed to be the result of the altered streaming of ions through the channel or reflect the difference in time scale of the two assays [75].

Probing the Role of the Arginine Cluster

Arginines 42, 82 and 132 have been implicated as the pH sensor for the voltage gating mechanism [64,75]. To determine the importance of the arginine cluster in the titration of the channel size switch, I studied the OmpF mutant R132L porin. My BLM experiments using R132L porin show a pattern of channel distribution similar to wild type OmpF (Figure 8, D and E). If the arginine cluster is the pH sensor for the channel size switch, then R132L is not a critical part of that behavior.

DISCUSSION

The temperature stability of mutant porins has been used as a probe to identify mutations that had dramatic effects upon porin structure [97,98,101]. For the most part, the porin mutants investigated in this study are only slightly destabilized with respect to temperature in comparison to wild type OmpF (Table II). The greatest effect upon temperature stability was observed for the mutant D113G. This suggests that the side chain of D113 is more critical to the overall stability of the protein than the residues 114-129, which are deleted in the porin of OC1555. However, this experiment does not differentiate between the charge on the side chain of D113 and the backbone conformational constraints caused by the R-group which are absent in the D113G mutant. This mutation affects the structural integrity of OmpF, but that does not mean that this residue is involved in any conformational shifts.

In the crystal structure of OmpF, the side chains of D113 and Y106 are arranged at a close distance with angles which are highly favorable for a hydrogen bond. The lessened temperature stability of D113G and Y106F may reflect the loss of the stabilizing hydrogen bond that the two share in the crystal structure. However, the Y106F mutation is no more destabilizing to OmpF than the other mutations, suggesting that the hydrogen bond interaction observed in the crystal structure is not as critical for the stability of the protein as is the individual side chain of D113. The residue, D113, is located on Loop 3, indicating that the loop plays a role in the structural integrity of OmpF.

The original model for the pH dependent size switch explained the DEPC modification effect on channel size as the result of a direct modification of the pH sensor. It has been shown that the mutant H21T had no effect on the pH titration of the voltage

39

gate [90], and in my studies I have shown that the mutation H21A did not alter the pH-dependent change in channel size. H21A OmpF porin is affected by DEPC-modification in the same way as wild type OmpF. The carbethoxylated porin is locked into large channel, regardless of pH. Histidine 21 is neither the pH sensor, nor the site of DEPC modification.

Y106F is insensitive to the addition of DEPC, and is capable of forming small channels at low pH even after the modification reaction. This evidence suggests that Y106 is the site of the DEPC modification responsible for locking the protein into the large channel conformation. However, Y106 is not a likely candidate for the pH sensor of the channel size switch. For a tyrosine side chain to be the donor in a hydrogen bond, the hydroxyl must be protonated. The crystal structure of OmpF was solved at basic pH [52]. The proposed hydrogen bond interaction between D113 and Y106 in the crystal structure of OmpF suggests that the hydroxyl of Y106 is still protonated at basic pH, implying that it does not titrate over the neutral pH range. This shows that Y106 is not a candidate for the titratable residue in the pH sensor for the switch in channel size.

The voltage gating of porin has also been shown to have a pH-dependent behavior [75,80]. The channel gates to a closed state in a voltage dependent manner, with the channels closing more readily (i.e., at lower voltages) when measured at acidic pH than they do at basic pH [75,80]. The titration midpoint of this gating activity is at approximately neutral pH [75], similar to the titration of channel size [87]. The arginine cluster has been implicated as the pH sensor for voltage gating because point mutants in the cluster remove the pH sensitivity [64,75]. The close packing of R42, R82 and R132 is suggested to lower their pK_a's from 12 to 7 [52,64], and this is supported by

macroscopic-based calculations utilizing the Poisson-Boltzmann equation [64]. However, the point mutation D113G also removed the pH sensor for the voltage gate [75], which indicates that pH sensitivity of the voltage gate includes more than just the arginine cluster. Furthermore, the observed effects of these point mutations on the pH sensitivity of voltage gating may indicate a general disruption of that activity, and these residues may not be directly related to the titratable element of the pH sensor for the voltage gate.

There is evidence suggesting that the same pH sensor may be involved in both the voltage gate and the channel size switch. The pH sensor for each activity titrates in the neutral pH range [75,87]. It has also been noted that high voltage tends to increase the amount of small channels observed at high pH [102]. Since the titratable group involved in the size switch is sensitive to voltage, the two activities may be linked, so that the pH sensor for the voltage gating and the channel size switch are coupled. The pH sensitivity of the voltage gate may reflect the differing voltage gating propensities between the large and the small channel conformational substates instead of the gating and the channel size each having their own pH sensor. Then the pH sensitivity of the voltage gate would be due to the titration of the channel size rather than a direct titration of the gating activity.

The residue(s) that comprises the pH sensor for the channel size switch, is still unknown. The histidine is not the pH sensor and neither is the DEPC-modifiable tyrosine. Likewise, the data does not support the arginine cluster as the pH sensor for the channel size switch. OmpF R132L porin has a wild type distribution of channel sizes, with small channels being observed at acidic pH and large channels at basic pH (Figure 8, D and E). This indicates that the pH sensor is intact for the mutant porin R132L. And in

a similar experiment, it has been shown that the mutant R82C retains the wild type channel size distribution with pH [103], which further refutes a model utilizing the arginine cluster as the pH sensor for the channel size switching mechanism. For similar charge to neutral mutants, R132C and R82C, the voltage gate's pH sensitivity is removed [75]. This data is in conflict with a model in which the pH sensor for the size switch and the voltage gate are coupled. It would be expected that a mutation, which removed the titration of the voltage gate, would also affect the pH sensor of the channel size switch. If the pH sensitivity of the two activities are coupled, then it is unlikely that the arginine cluster is the pH sensor for either the size switch or the voltage gate.

Since the DEPC modification is not directly modifying the pH sensor for the size switch, then the explanation for the effects of modification on porin functionality must be related to the structure of the modified residue. The carbethoxylated tyrosine (Figure 10) is no longer capable of being the donor in the hydrogen bond. However, the effect of modification upon the channel size is not due to the loss of Y106's hydrogen bonding capacity because the mutant Y106F can still form stable small channel (Figure 7E) even though the phenylalanine cannot be a donor in a hydrogen bond. It is possible that the modified residue has introduced a stabilizing interaction in the large channel conformation that is responsible for a highly stable large channel. Another, more likely possibility is that the bulky carbethoxylated tyrosine is large enough to be a steric hindrance to the formation of small channel. The channel is locked into large conformation by DEPC modification because it is blocked from forming small channel. This explanation implies that Y106 must be part of a conformational rearrangement to shift the channel from the large channel to the small channel conformational substate.

Figure 10. The structures of diethyl pyrocarbonate (DEPC) and carbethoxylated tyrosine, and two views of DEPC-modified-Y106 in the protein, show the bulky modification that locks OmpF into the large channel conformation. The carbethoxyl addition to the side chain of Y106 is merely being modeled; the structure has not been minimized or altered except for the addition of the modifying group. The channel is being viewed from a position inside the channel, near the arginine cluster, looking across the channel at Loop 3 (A), and also from the extracellular space (B). Loop 3 is colored yellow, with the α-helical portion being shaded green. The residues of the two ribbon structures [52] pictured, are shown as ball and stick models without hydrogens. The arginines (R42, R82, R132, and R140) are yellow, the lysine (16K) is green, the aspartates (D107 and D113) are red, the tyrosine (Y106) is blue and the carbethoxy addition to Y106 is black. The structures of DEPC (C) and carbethoxylated tyrosine (D) are ball and stick models with gray hydrogens, green carbons, red oxygens, and blue nitrogens.
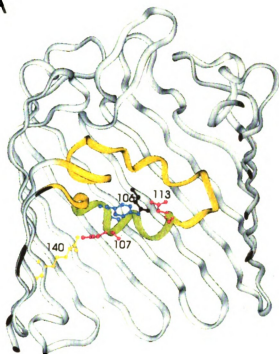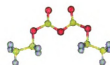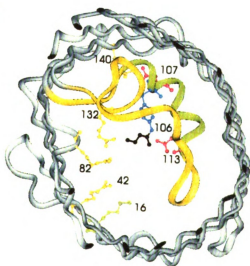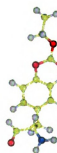
Figure 10

The residue, Y106, is on the short α-helical region of Loop 3, suggesting that the

loop may be involved in the channel size switch. The deletion mutant, OC1555 ($\Delta114$-

129), removes most of Loop 3 except for a portion that includes the α-helix. OC1555

shows a slight decrease (<15%) in the small channel size observed at acidic pH, and a

much greater decrease (>60%) in the size of the large channels observed at basic pH

(Table 3). The differential effect upon large and small channel suggests that the deleted

portion of Loop 3 in the mutant is more significant for determining the size (λ/σ) of the

large channel than the small channel as observed in the BLM results. Apparently, the

components of the protein that define small channel size vary from those that define the

size of the large channel substate. This is consistent with the suggested model for the

channel size switch [87,88], in which there is a conformational rearrangement between

the large channel and the small channel substates of OmpF.

While the pH sensor for the size switch has not been identified, Loop 3 has been

implicated in the conformational switch between the two channel size substates. The

DEPC modification experiments have shown that Y106 is involved in the conformational

shift to form small channel, so it is likely that Loop 3 undergoes a physical alteration in

the conformational shift between the large and small channel substates. Loop 3 has six

acidic groups on it, which are the only charged residues on the loop other than R132.

The deletion mutant OC1555 removes four of the six charges and is still capable of

forming small channel. One of the two remaining charges has been mutated, D113G, and

has been shown to form small channel at low pH [103], as well as large channels at basic

pH (Figure 8A). That leaves only D107 as a potentially critical acidic group to interact

with a pH sensor. In the crystal structure, presumably the large channel conformation,

D107 interacts closely with R140 of the wall of the barrel, away from the eyelet structure of the channel (Figure 11) [52]. Both D107 and R140 are highly conserved among PhoE, OmpC and OmpF [42]. D107 is on the α–helical portion of Loop 3. If the Y106 side chain is moving, as implied from the DEPC experiment, then that motion would likely have an effect on the entire helix. FTIR shows that the amount of secondary structure does not change over the given pH range [88], which suggests that the α-helix remains intact at both acidic and basic pH. At acidic pH, a movement of the entire α–helix could expose the negatively charged D107 to the positively charged sensor, using that interaction as a stabilizing force which could move the helical portion of Loop 3 into the eyelet region. This new conformation of Loop 3 would result in a constricted eyelet.

Figure 11. Cutaway ribbon diagrams of OmpF [52] focused on the positions of D107, R140 and K16. Loop 3 is turquoise, with the portion of the loop deleted in the OC1555 mutation (Δ114-129) shaded in purple. The displayed residues are modeled in a ball and stick style, without hydrogens. The arginines (R42, R82, R132 and R140) are yellow, the lysine (K16) is green, the aspartate residues (D107, D113 and D117) are red and the tyrosine (Y106) is blue. The protein is being viewed from the extracellular space (A), the periplasm (B), and from a position inside the channel across from Loop 3, placing the viewer near the arginine cluster (C).
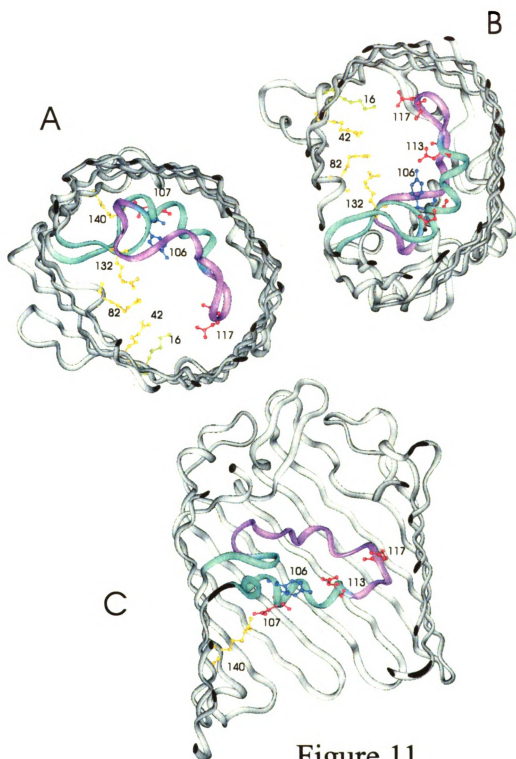
A

B

C

Figure 11

SUMMARY AND PERSPECTIVES

The pH sensor for the mechanism of the channel size switch has not been identified. The evidence suggests that neither the conserved histidine, nor the arginine cluster is critical components of the pH sensor. Other residues in the channel have been proposed to titrate around neutral pH, namely K16 and K80 [64]. K16 is conserved among OmpF, OmpC and PhoE [42], so it is a candidate for the pH sensor of the channel size switch. K16 is also located near the arginine cluster, directly across the channel from Loop3, putting it in a position to possibly influence the structure of that loop (Figure 11).

The only structural insight into the formation of small channel has been the involvement of residue Y106. The DEPC experiments in this study suggest that Y106 is involved in a structural rearrangement that occurs in the formation of the small channel conformation. This conformational shift would likely include a local rearrangement of Loop 3, which is somehow controlled by pH. Site-directed mutagenesis could be used to test the proposed model for the channel size switch. The role of Loop 3 could be better evaluated if the entire loop were deleted, or at least the portion of the loop which has not been deleted up to this point. The roles of D107 and R140 could be tested by the mutation R140D or R140E, which would destabilize their interaction as observed in the crystal structure of OmpF but would not interfere with the proposed interaction between D107 and the positively charged sensor of the small channel conformation. The converse of that experiment, would be to make a double mutant of D107R and R140D. This inversion of the interaction could lock the porin in the large channel configuration since the positively charged arginine at 107 would not be a stabilizing interaction with the

positively charged sensor at acidic pH. In order to test the role of K16 as the pH sensor, a charge to neutral mutation such as K16A would remove the titratable nature of that residue. If K16 is the pH sensor, then the channel would be locked into the large channel conformation because it lacks the electrostatic driving force that stabilizes the small channel structure. Ultimately, the small channel conformation would need to be confirmed through a structural technique such as multidimensional NMR or protein crystallography. If K16 is the pH sensor, then the drop in the pKa of its side chain must be due to its local environment. A mutation that altered the local environment of K16, to shift its pKa back up to 10, would result in a protein that is locked into the small channel conformation. That protein could then be crystallized under the required conditions to solve the structure of OmpF for the small channel conformation.

The mitochondrial porin, VDAC (voltage dependent anion channel), also has two channel sizes [104-106] which are influenced by pH [107]. The conformational shift between the two channel sizes of VDAC is driven by voltage, with the large channel being present at very low voltage and the small channel being observed at higher voltages [104-107]. The voltage required for the formation of the small channel varies directly with pH [107]. Lowering the pH decreases the required voltage for the change between the two channel sizes, and at basic pH, the size switch of VDAC is desensitized to voltage [107]. In a similar manner, it has been observed that high voltage can stabilize the small channel conformation of the porins of *E. coli* [102]. The interwoven effects of pH and voltage upon the channel sizes of VDAC and the porins of *E. coli* suggest that the mechanisms for controlling channel size may be similar between the two groups of proteins.

The effects of pH upon the channel size and voltage gating mechanism of the porins of *E. coli* fit into an overall pattern for the control of diffusion across the outer membrane. The control of diffusion across the outer membrane occurs on two levels. One level of control is the regulated expression of porin, and the other is the immediate functional response of porin to the environmental conditions. Enteric bacteria exist in either the gut of a host organism or in the water supply. The pattern of porin expression reflects the conditions of the environment. The channel formed by OmpC is approximately one half the cross-sectional area (λ/σ) of that of OmpF. The expression of OmpF is favored by growth conditions normally found outside the host, where its larger channel would be advantageous for nutrient uptake. Conversely, environmental conditions that are found inside the host, i.e. high temperature, high osmolarity and low pH, favor the synthesis of the smaller channel of OmpC. Inside the gut of the host, nutrients are much more concentrated and nutrient uptake can readily occur with a smaller channel [11,12]. There is evidence that OmpC provides the bacterium with better resistance to some antibiotics [108], and it is proposed that the expression pattern of the two porins reflects an adaptation of the bacterium to increase resistance to host defense mechanisms [4,108].

The change in gene expression for outer membrane proteins is a relatively slow process, requiring the bacteria to replicate to fully replace OmpF with OmpC. The responsive nature of the porin structure to environmental conditions complements its pattern of gene expression. The pH-induced switch in porin channel size favors a larger channel when the cells are in ponds or streams, while in the gut, the lower pH stabilizes the smaller channel size of the protein. This decreased size reduces the permeability of

the outer membrane, presumably as a defensive mechanism to survive the harsh conditions of the gut. The small channel of OmpF is approximately the size of the large channel of OmpC, and it is logical that the small channel of OmpC provides even greater protection from deleterious agents. The voltage gate of OmpF is far more sensitive to acidic conditions than that of OmpC [75]. Perhaps this is a mechanism to further decrease the permeability of the outer membrane and help the invading bacteria to survive inside the host until the OmpF in the outer membrane can be replaced with OmpC.

Although this study has revealed some insight into the pH dependent size switch of porin, the mechanism for both the channel size switch and the voltage gate remain unknown. The structure-function studies of the porins of Gram-negative bacteria will provide insight into the mechanistic controls that influence the permeability of the outer membrane. Given the similarity between the porins and VDAC, porin studies may provide a more complete understanding of the functionality for both of these channel-forming proteins.

REFERENCES

1. Kellenberger, E., and Ryter, A. (1958) *J. Biophys. Biochem. Cytol.* **4**, 323-326.

2. Cronan, J.E. Jr., Gennis R.B., and Maloy, S.R. (1987) in *Escherichia coli and Salmonella typhimurium Cellular and Molecular Biology* (Neidhardt, F.C., Ingraham, J.L., Low, K.B., Magasanik, B., Schaechter, M., and Umbarger, H.E., eds.) pp. 31-55 American Society for Microbiology, Washington.

3. Brass, J.M. (1986) *Curr. Top. Microbiol. Immunol.* **129**, 1-92.

4. Tam, R., and Saier, M.H., Jr. (1993) *Microbiol. Rev.* **57**, 320-346.

5. Oliver, D.B. (1996) in *Escherichia coli and Salmonella typhimurium Cellular and Molecular Biology* (Neidhardt, F.C., Curtiss, Roy, Ingraham, J.L., Lin, E.C.C., Low, K.B., Magasanik, B., Reznikoff, W.S., Riley, M., Schaechter, M., and Umbarger, H.E., eds.) pp. 88-103 American Society for Microbiology, Washington.

6. Park, J.T. (1996) in *Escherichia coli and Salmonella typhimurium Cellular and Molecular Biology* (Neidhardt, F.C., Curtiss, Roy, Ingraham, J.L., Lin, E.C.C., Low, K.B., Magasanik, B., Reznikoff, W.S., Riley, M., Schaechter, M., and Umbarger, H.E., eds.) pp. 48-57 American Society for Microbiology, Washington.

7. Hancock, R.E.W. (1984) *Ann. Rev. Microbiol.* **38**, 237-264.

8. Lugtenberg, B., and van Alphen, L. (1983) *Biochim. Biophys. Acta.* **737**, 51-115.

9. Nikaido, H., and Nakae, T. (1979) *Adv. Microbiol. Physiol.* **20**, 163-250.

10. Osborn, M.J., Gander, J.E., Parisi, E., and Carson, J. (1972) *J. Biol. Chem.* **247** 3962-3972.

11. Nikaido, H., and Vaara, M. (1985) *Microbiol. Rev.* **49**, 1-32.

12. Nikaido, H. (1996) in *Escherichia coli and Salmonella typhimurium Cellular and Molecular Biology* (Neidhardt, F.C., Curtiss, Roy, Ingraham, J.L., Lin, E.C.C., Low, K.B., Magasanik, B., Reznikoff, W.S., Riley, M., Schaechter, M., and Umbarger, H.E., eds.) pp. 29-47 American Society for Microbiology, Washington.

13. Takeuchi, Y., and Nikaido, H. (1981) *Biochemistry* **20**, 523-529.

14. Nikaido, H., Takeuchi, Y., and Nakae, T. (1977) *Biochim. Biophys. Acta* **465**, 152-164.

15. Labischinski, H., Barnickel, G., Bradaczek, H., Naumann, D., Rietschel, E.T., and Giesbrecht, P. (1985) *J. Bacteriol.* **169**, 9-20.

16. Labischinski, H., Naumann, D., Schulz, C., Kusumoto, S., Shiba, T., Rietshel, E.T., and Giesbrecht, P. (1989) *Eur. J. Biochem.* **179**, 659-665.

17. Vaara, M., Plachy, W.Z., and Nikaido, H. (1990) *Biochim. Biophys. Acta* **1024**, 152-158.

18. Makela, P.H., Bradley, D.J., Brandis, H., Frank, M.M., Hahn, H., Henkel, W., Jann, K., Marse, S.A., Robbins, J.B., Rosenstreich, L., Smith, H., Timmis, K., Tomasz, A., Turner, M.J., and Wiley, D.C. (1980) in *The molecular basis of microbial pathogenity* (Smith, H., Skehel, J.J., and Turner, M.J., eds) pp 174-197 Verlag Chemie GmbH, Weinheim, Federal Republic of Germany.

19. Vaara, M. (1993) *Antimicrob. Agents Chemother.* **37**, 2255-2260.

20. Hirvas, L., Koski, P., and Vaara, M. (1991) *EMBO J.* **10**, 1017-1023.

21. MacGregor, C.H., Bishop, C.W., and Blech, J.E. (1979) *J. Bacteriol.* **137**, 574-583.

22. Nishijima, M., Nakaike, S., Tamori, Y., and Nojima, S. (1977) *Eur. J. Biochem.* **73**, 115-124.

23. Hantke, K. (1976) *FEBS Lett.* **70**, 109-112.

24. Neilands, J.B. (1982) *Ann. Rev. Microbiol.* **36**, 285-309.

25. Braun, V. and Rehn, K. (1969) *Eur. J. Biochem.* **10**, 426-438.

26. Henning, U., Hohn, B., and Sonntag, I. (1973) *Eur. J. Biochem.* **39**, 27-36.

27. Sugawara, E., and Nikaido, H. (1992) *J. Biol. Chem.* **267**, 2507-2511.

28. Nikaido, H., Bavoil, H.P., and Hirota, Y. (1977) *J. Bacteriol.* **132**, 1045-1047.

29. Benz, R. (1988) *Annu. Rev. Microbiol.* **42**, 359-393.

30. Cowan, S.W., and Schirmer, T. (1994) *Bacterial Cell Wall. New Comprehensive Biochemistry*, vol. 27 (Ghuysen, J.-M., and Hakenbeck, R., eds.) Elsevier, Amsterdam.

31. Nikaido, H. (1992) *Mol. Microbiol.* **6**, 435-442.

32. Schulz, G.E. (1993) *Curr. Opin. Cell Biol.* **5**, 701-707.

33. Bavoil, P., Nikaido, H., and von Meyenburg, K. (1977) *Mol. Gen. Genet.* **158**, 23-33.

34. Graeme-Cook, K.A., May, G., Bremer, E., and Higgins, C.F. (1989) *Mol. Microbiol.* **3**, 1287-1294.

35. Pratt, L.A., Hsing, W., Gibson, K.E., and Silhavy, T.J. (1996) *Mol. Microbiol.* **20**, 911-917.

36. Heyde, M., Lazzaroni, J.-C., Magnouloux-Blanc, B., and Portalier, R. (1988) *FEMS Micro. Lett.* **52**, 59-66.

37. Heyde, M., and Portalier, R. (1987) *Mol. Gen. Genet.* **208**, 511-517.

38. Graeme-Cook, K.A. (1991) *FEMS Micro. Letters* **79**, 219-224.

39. Lugtenberg, B., Peters, R., Bernheimer, H., and Berendsen, W., (1976) *Mol. Gen. Genet.* **147**, 251-262.

40. Benz, R. (1988) *Ann. Rev. Microbiol.* **42**, 359-393.

41. Benz, R. Schmid, A., and Hancock, R.E. (1985) *J. Bacteriol.* **162**, 722-727.

42. Jeaneur, D., Lakey, J.H., and Pattus, F. (1991) *Mol. Microbiol.* **5**, 2153-2164.

43. Benedicte, D., Rosenbusch, J.P., and Pattus, F. (1987) *FEBS Lett.* **220**, 136-142.

44. Szmelcman, S., and Hofnung, M. (1975) J. *Bacteriol.* **124**, 112-148.

45. Palva, E.T. (1978) *J. Bacteriol.* **136**, 286-294.

46. Heyde, M., and Portalier, R. (1987) *Mol. Gen. Genet.* **208**, 511-517.

47. Overbeeke, N., and Lugtenberg, B. (1980) *FEBS Lett.* **112**, 229-232.

48. Bauer, K., van der Ley, P., Benz, R., and Tommassen, J. (1988) *J. Biol Chem.* **263**, 13046-13053.

49. Nakae, T. (1976) *Biochem. Biol. Res. Comm.* **71**, 877-884.

50. Schnaitman, C.A. (1974) *J. Bacteriol.* **118**, 454-464.

51. Datta, D.B., Kramer, C., and Henning, U. (1976) *J. Bacteriol.* **128**, 834-841.

52. Cowan, S.W., Schirmer, T., Rummel, G., Steiert, M., Ghosh, R., Paupit, R.A., Jansonius, J.N., and Rosenbusch, J.P. (1992) *Nature* **258**, 727-733.

53. Weiss, M.S., and Schulz, G.E. (1993) *J. Mol. Biol.* **231**, 817-824.

54. Weiss, M.S., and Schulz, G.E. (1992) *J. Mol. Biol.* **227**, 493-509.

55. Weiss, M.S., Kreusch, A., Schiltz, E., Nestel, U., Welte, W., Weckesser, J., and Schulz, G.E. (1991) *FEBS Lett.* **280**, 379-382.

56. Schiltz, E., Kreusch, A., Nestel, U., and Schulz, G.E. (1991) *Euro. J. Biochem.* **199**, 587-594.

57. Schulz, G.E. (1996) *Curr. Opinions in Struct. Biol.* **6**, 485-490.

58. Cowan, S.W., and Rosenbusch, J.P. (1994) *Science* **264**, 914-916.

59. Benz, R. (1985) *CRC Curr. Rev. Biochem.* **19**, 145-190.

60. de Pinto, V., and Palmier, F. (1992) *J. Bioenerg. Biomembr.* **24**, 21-26.

61. Fuks, B., and Hombles, F. (1995) *J. Biol. Chem.* **270**, 9947-9952.

62. Hancock, R.E., Decad, G.M., and Nikaido, H. (1979) *Biochim. Biophys. Acta* **554**, 323-331.

63. Schulz, G.E. (1995) Biochemistry of the Cell Membrane (Papa, S., and Tager, J.M., eds.) pp. 327-338 Birkhauser Verlag, Basel/Switzerland.

64. Karshikoff, A., Spassov, V., Cowan, S.W., Ladenstein, R., and Schirmer, T. (1994) *J. Mol. Biol.* **240**, 372-384.

65. Benson, S.A., and Decloux, A. (1985) *J. Bacteriol.* **161**, 361-367.

66. Misra, R., and Benson, S.A. (1988) *J. Bacteriol.* **170**, 528-533.

67. Misra, R., and Benson, S.A. (1988) *J. Bacteriol.* **170**, 3611-3617.

68. Benson, S.A., Occi, J.L.L., and Sampson, B.A. (1988) *J. Mol Biol.* **203**, 961-970.

69. Schindler, H., and Rosenbusch, J.P. (1978) *Proc. Nat. Acad. Sci. USA* **75**, 3751-3755.

70. Benz, R., and Bauer, K. (1988) *Eur. J. Biochem.* **176**, 1-19.

71. Benz, R., Janko, K., and Lauger, P. (1979) *Biochim. Biophys. Acta* **511**, 238-247.

72. Benz, R., Janko, K., Boos, W., and Lauger, P. (1978) *Biochim. Biophys. Acta* **511**, 305-319.

73. Brunen, M., Engelhardt, H., Schmidt, A., and Benz, R. (1992) *J. Bacteriol.* **173**, 4182-4187.

74. Nikaido, H. (1992) *Mol. Microbiol.* **6**, 435-442.

75. Saint, N., Lou, K.C., Widmer, C., Luckey, M., Schirmer, T., and Rosenbusch, J.P. (1996) *J. Biol. Chem.* **271**, 20676-20680.

76. Jeanteur, D., Schirmer, T., Fourel, D., Simonet, V. Rummel, G., Widmer, C., Rosenbusch, J.P., Pattus, F., and Pages, J. (1994) *Proc. Nat. Acad. Sci. USA* **91**, 10675-10679.

77. Schirmer, T., Keller, T.A., Wang, H., and Rosenbusch, J.P. (1995) *Science* **267**, 512-514.

78. Schindler, M., and Rosenbusch, J.P. (1981) *Proc. Nat. Acad. Sci. USA* **78**, 2302-2306.

79. Dargent, B., Hofmann, W., Pattus, F., and Rosenbusch, J.P. (1986) *EMBO J.* **5**, 773-778.

80. Xu, G., Shi, B., McGroarty, E.J., and Tien, H.T. (1986) *Biochim. Biophys. Acta* **862**, 57-64.

81. Declour, A.H., Martinac, B., Adler, J. and Kung, C. (1989) *J. Membr. Biol.* **112**, 267-275.

82. Stock, J.B., Rauch, B., and Rosemann, S. (1977) *J. Biol. Chem.* **252**, 7850-7861.

83. Sen, K., Hellman, J., and Nikaido, H. (1988) *J. Biol. Chem.* **263**, 1182-1187.

84. Lakey, J.H., Watts, J.P. and Lea, E.J.A. (1985) *Biochim. Biophys. Acta* **817**, 208-216.

85. Declour, A.H., Adler, J., Kung, C., and Martinac, B. (1992) *FEBS Lett.* **304**, 216-220.

86. dela Vega, A.L., and Declour, A.H. (1995) *EMBO J.* **14**, 6058-6065.

87. Todt, J.C., Rocque, W.J., and McGroarty, E.J. (1992) *Biochemistry* **31**, 10471-10478.

88. Todt, J.C., and McGroarty, E.J. (1992) *Biochemistry* **31**, 10479-10482.

89. Miles, E.W. (1977) *Methods Enzymol.* **47**, 431-442.

90. Saint, N., Prilipov, A., Hardmeyer, A., Lou, K.-C., Schirmer, T., and Rosenbusch, J.P. (1996) *Biochim. Biophys. Acta* **223**, 118-122.

91. Schindler, M., and Rosenbusch, J.P. (1982) *J. Cell Biol.* **92**, 742-746.

92. Cole, S.T., Sonntag, I., and Henning, U. (1982) *J. Bacteriol.* **149**, 145-150.

93. Hiser, C. (1996), unpublished.

94. Roundtree, J.D., and Hiser, C. (1997), unpublished.

95. Benson, S. personal communication.

96. Laemmli, U.K. (1970) *Nature* **227**, 680-685.

97. Rocque, W.J., and McGroarty, E.J. (1990) *Biochemistry* **29**, 5344-5351.

98. Rocque, W.J., and McGroarty, E.J. (1989) *Biochemistry* **28**, 3738-3743.

99. Bindslev, N., and Wright, E.M. (1984) *J. Membrane Biol.* **81**, 159-170.

100. Lou, K.-L., Saint, N., Prilipov, A., Rummel, G., Benson, S.A., Rosenbusch, J.P., and Schirmer, T. (1996) *J. Biol. Chem.* **271**, 20669-20675.

101. Lakey, J.H., Lea, E.J.A., and Pattus, F. (1991) *FEBS Lett.* **278**, 31-34.

102. McGroarty, E.J. unpublished.

103. Todt, J.T. (1992) unpublished.

104. Manella, C.A. (1992) *TIBS* **17**, 315-320.

105. Manella, C.A., Forte, M., and Colombini, M. (1992) *J. Bioenerg. Biomembr.* **24**, 7-19.

106. Guo, X.W., and Manella, C.A. (1993) *Biophys. J.* **64**, 545-549.

107. Ermishkin, L.N., and Mirzabekov, T.A. (1990) *Biochim. Biophys. Acta* **1021**, 161-168.

108. Medeiros, A.A., O'Brien, T.F., Rosenberg, E.Y., and Nikaido, H. (1987) *J. Infect. Dis.* **156**, 751-757.